Polyhedron 28 (2009) 3101–3109

Contents lists available at ScienceDirect

Polyhedron

journal homepage: www.elsevier.com/locate/poly

Transition metal complexes of *N*-1-tosylcytosine and *N*-1-mesylcytosine

Aleksandar Višnjevac [a], Nikola Biliškov [b], Biserka Žinić [b,*]

[a] Division of Physical Chemistry, Ruđer Bošković Institute, Bijenička 54, 10000 Zagreb, Croatia
[b] Division of Organic Chemistry and Biochemistry, Ruđer Bošković Institute, Bijenička 54, 10000 Zagreb, Croatia

ARTICLE INFO

Article history:
Received 14 May 2009
Accepted 24 June 2009
Available online 3 August 2009

Keywords:
Transition metal complexes
N-1-Substituted cytosine
X-ray diffraction
IR spectroscopy
NMR spectroscopy

ABSTRACT

The syntheses as well as chemical and X-ray structural characterization of dichlorobis[1-(*p*-toluenesulfonyl)cytosine]copper(II) (**2**), its solvated pseudopolymorph containing two methanol molecules (**3**), dichlorobis[1-(*p*-toluenesulfonyl)cytosine]cadmium(II) (**4**), 1-methanesulfonylcytosine (**6**) and its copper complex dichlorobis(1-methanesulfonylcytosine)copper(II) (**7**) are described. In addition, spectroscopic studies of dichlorobis[1-(*p*-toluenesulfonyl)cytosine]cobalt(II) (**5**), as well as of dichlorobis(1-mesylcytosine)cadmium(II) (**8**) are presented. Pseudopolymorphs **2** and **3**, as well as their 1-mesylcytosine analog **7**, reveal square-planar coordination spheres, almost ideal in the case of **2**, but considerably distorted in the case of **3** and **7**. In all cases, the Cu(II) ion is coordinated by two endocyclic N3 atoms from two ligand molecules and by two chlorine atoms. The analogous coordination sphere was found in complex **4**, where Cd(II) lies in the center of a slightly distorted tetrahedron formed by two endocyclic N3 atoms and by two chlorine atoms.

1. Introduction

The interaction of various metal ions with nucleobases as structural elements of nucleic acids is of considerable interest for a number of reasons. Metal ions participate in nucleic acid–enzyme interactions during replication and transcription [1] and their role in inducing carcinogenesis and mutagenesis is very well documented [2]. It is also well known that the affinity of some transition metal ions to bind at a specific site of the nucleotide molecule has a deeper impact on the conformation and overall stability of the DNA molecule in solution [3]. It was found that Cu(II), Hg(II) and Cd(II), due to their high affinity for coordination to nitrogen sites of the nucleotide base, help break the hydrogen bonds involved in nucleobase pairing and, consequently, disrupt the structure of the double helix. On the other hand, ions like Co(II), Zn(II) and Mg(II), which prefer to bind to phosphate groups, leave the hydrogen bonding arrangements inside the DNA structure intact and thus do not destabilize the DNA structure [4].

To study the latter phenomenon, in our current study we report on the Cu(II), Cd(II) and Co(II) coordination to 1-(*p*-toluenesulfonyl)cytosine (**1**) [1-tosylcytosine or TsC] and 1-methanesulfonylcytosine (**6**) [1-mesylcytosine or MsC], two ligand compounds belonging to the series of *N*-sulfonylpyrimidine derivatives which reveal intriguing biological activity both *in vitro* and *in vivo* and are the subject of our comprehensive studies [5]. Besides their biological activity, these compounds are also a very good and simple model for investigating the coordination properties of *N*-1 substituted pyrimidine nucleobases, as reported in our previous paper [6] and herein. According to the above cited previous reports, Cu(II) and Cd(II) readily formed complex compounds with our ligands, while the formation of Co(II), and Ni(II) complexes with the same ligands was not easy or was impossible to achieve.

2. Experimental

2.1. General remarks

^{1}H and ^{13}C NMR spectra were recorded in DMSO-d_6 and CD_3CN on Bruker AV 300 and 600 MHz spectrometers using CD_3CN (δ = 1.94 ppm) or DMSO-d_6 (δ = 2.5 ppm) as internal standards. Elemental analyses were done on a Perkin–Elmer 2400 Series II CHNS analyzer. Infrared spectra were collected using an ABB Bomem MB102 spectrometer. CsI pellets of all samples were prepared in order to record spectra at room temperature as an average of 10 co-added scans with a nominal resolution of 4 cm^{-1}. Temperature dependent IR spectra and thermogravimetry data are in the Supplementary material (general Figs. S1a and S1b). Positive ion mass spectra were acquired using a Micromass Q-Tof2 hybrid quadrupole time-of-flight mass spectrometer, equipped with a Z-spray interface, over a mass range of 100–2000 Da, with a scan time of 1.5 s and an interscan delay of 0.1 s in the continuum mode. NaCsI was used as the external mass calibrant lock mass. Ionization was achieved with a capillary voltage of 3.50 kV, a cone voltage of 30 V,

* Corresponding author. Tel.: +385 1 4561066; fax: +385 1 4680195.
E-mail address: bzinic@irb.hr (B. Žinić).

0277-5387/$ - see front matter © 2009 Elsevier Ltd. All rights reserved.
doi:10.1016/j.poly.2009.06.088

and with cone and desolvation gas flows of 5–10 and 500 L/h, respectively (details and spectra Figs. S2–S12 in Supplementary material).

2.2. Preparation of the ligands

A mixture of cytosine (1 mmol) and *N,O*-bis(trimethylsilyl)acetamide (BSA) (3 mmol) was heated under reflux in dry acetonitrile (3.3 mL) for 1 h. The solution was cooled to 0 °C and sulfonyl chloride (1.2 mmol) was added. The reaction mixture was heated for 16 h at 80 °C, cooled and treated with a small amount of methanol. The resulting solid was filtered off and recrystallized.

2.2.1. 1-(p-Toluenesulfonyl)cytosine (**1**)

Synthesis of ligand **1** was performed according to the procedure reported by Kašnar-Šamprec et al. [7]. [^{1}H NMR (DMSO-d_6) δ/ppm: 8.14 (d, 1H, $J_{6,5}$ = 7.8 Hz, H-6), 7.95 (brd, 2H, NH_2), 7.87 (d, 2H, $J_{b,c}$ = 8.1 Hz, Ph-b), 7.46 (d, 2H, $J_{c,b}$ = 8.1 Hz, Ph-c), 5.98 (d, 1H, $J_{5,6}$ = 7.8 Hz, H-5), 2.42 (s, 3H, CH_3); ^{13}C NMR (DMSO-d_6) δ/ppm: 166.27 (s, C-4), 151.22 (s, C-2), 145.61 (s, Ph-d), 139.73 (d, C-6), 134.47 (s, Ph-a), 129.80 (d, Ph-c), 129.02 (d, Ph-b), 97.50 (d, C-5), 21.20 (q, CH_3)]. *Anal.* Calc. for $C_{11}H_{11}N_3O_3S$ (M_r = 265.30): C, 49.80; H, 4.18; N, 15.84. Found: C, 50.09; H, 4.02; N, 15.89%.

Additional data for 1-(*p*-toluenesulfonyl)cytosine (**1**): ^{1}H NMR (CD_3CN) δ/ppm: 8.13 (d, 1H, $J_{6,5}$ = 7.9 Hz, H-6), 7.92 (brd, 2H, $J_{b,c}$ = 8.4 Hz, Ph-b), 7.46 (d, 2H, $J_{c,b}$ = 8.0 Hz, Ph-c), 6.42 (brd 2H, NH_2), 5.98 (d, 1H, $J_{5,6}$ = 7.8 Hz, H-5), 2.49 (s, 3H, CH_3).

2.2.2. 1-Methanesulfonylcytosine (**6**)

1-Methanesulfonylcytosine (**6**) was prepared according to the literature method [8]. [^{1}H NMR (DMSO-d_6) δ/ppm: 8.21 (brs, 1H, NH), 8.05 (brs, 1H, NH), 7.87 (d, 1H, $J_{6,5}$ = 7.8 Hz, H-6), 5.96 (d, 1H, $J_{5,6}$ = 7.9 Hz, H-5), 3.63 (s, 3H, CH_3); ^{13}C NMR (DMSO-d_6) δ/ppm: 165.44 (s, C-4), 151.42 (s, C-2), 139.45 (d, C-6), 96.64 (d, C-5), 41.13 (q, CH_3)]. *Anal.* Calc. for $C_5H_7N_3O_3S$ (M_r = 189.20): C, 31.74; H, 3.73; N, 22.21. Found: C, 31.92; H, 4.01; N, 22.02%.

2.3. Preparation of the complexes

To a water or methanol solution of $MCl_2 \times nH_2O$ (1 equiv.), the 1-sulfonylcytosine ligand (2 equiv.) in methanol was added and the reaction mixture was left stirring. The solid product obtained by evaporation was filtered off, washed with methanol and dried.

2.3.1. Cu(1-TsC-N3)$_2$Cl$_2$ (**2**)

Starting materials: solutions of 1-(*p*-toluenesulfonyl)cytosine (**1**) (133 mg, 0.5 mmol) in methanol (23 mL), $CuCl_2 \times 2H_2O$ (43 mg, 0.25 mmol) in methanol (5 mL). The resulting dark green solution was left to slowly evaporate at room temperature in order to obtain high quality single crystals. After 7 days, two types of single crystals were present in the crystallization vessel – deep blue prisms (X-ray structure **2**) and turquoise plates [methanol solvate of **2**, X-ray structure **3** (**2** × $2CH_3OH$)]. After selection of single crystals suitable for X-ray diffraction experiments, the remaining crystals were filtered off and dried in vacuum to remove the methanol yielding 110 mg (66%) of the blue-green complex **2**: ^{1}H NMR (DMSO-d_6) δ/ppm: 8.25 (brs, 1H, H-6), 7.89 (brs, 2.5H, Ph-b + part of NH_2), 7.42 (brs, 3.5H, Ph-c + part of NH_2), 2.34 (brs, 3H, CH_3); ^{1}H NMR (CD_3CN) δ/ppm: 9.48 (brs, 1H), 8.71 (brs, 2H), 7.79 (brs, 2H), 2.59 (brs, 3H, CH_3); ^{13}C NMR (DMSO-d_6) δ/ppm: 143.22 (s, Ph-d), 132.13 (s, Ph-a), 127.58 (d, Ph-c), 126.75 (d, Ph-b), 19.27 (q, CH_3). *Anal.* Calc. for $C_{22}H_{22}Cl_2CuN_6O_6S_2 \times 2H_2O$ (M_r = 701.06): C, 37.69; H, 3.74; N, 11.99. Found: C, 37.29; H, 4.10; N, 11.74%. ESI-HRMS (*m*/*z*): $[M-TsC-Cl]^+$ ($C_{11}H_{11}N_3O_3SCuCl$): calc. 362.9506, found: 362.9494 (3.3 ppm); $[M-Cl]^+$ ($C_{22}H_{22}N_6O_6S_2CuCl$): calc. 628.0027, found: 627.9995 (5.1 ppm); $[M+TsC-Cl]^+$ ($C_{33}H_{33}N_9O_9S_3CuCl$): calc. 893.0548, found: 893.0547 (0.1 ppm).

2.3.2. Cd(1-TsC-N3)$_2$Cl$_2$ (**4**)

Starting materials: solutions of 1-(*p*-toluenesulfonyl)cytosine (**1**) (133 mg, 0.5 mmol) in methanol (23 mL), 2 M aqueous solution of $CdCl_2$ (0.125 mL, 0.25 mmol). The colorless solution was stirred overnight and was then left to evaporate at room temperature. After 4 days, colorless prisms were obtained. One transparent colorless crystal was picked for the X-ray diffraction study, and the remaining crystals were filtered off and dried in vacuum to give 131 mg (77%) of white powder **4**: ^{1}H NMR (DMSO-d_6) δ/ppm: 8.75 (brs, 1H, NH), 8.26 (brs, 1H, NH), 8.22 (d, 1H, $J_{6,5}$ = 8.0 Hz, H-6), 7.88 (d, 2H, $J_{b,c}$ = 8.3 Hz, Ph-b), 7.48 (d, 2H, $J_{c,b}$ = 8.1 Hz, Ph-c), 6.06 (d, 1H, $J_{5,6}$ = 8.0 Hz, H-5), 2.41 (s, 3H, CH_3); ^{1}H NMR (CD_3CN) δ/ppm: 8.19 (brd, 1H, H-6), 8.08 (brs, 1H, NH), 7.90 (brd, 2H, Ph-b), 7.43 (brd, 2H, Ph-c), 7.39 (brs, 1H, NH), 6.10 (brd, 1H, H-5), 2.45 (brs, 3H, CH_3); ^{13}C NMR (DMSO-d_6) δ/ppm: 163.35 (s, C-4), 148.38 (s, C-2), 146.02 (s, Ph-d), 140.38 (d, C-6), 133.29 (s, Ph-a), 129.71 (d, Ph-c), 129.01 (d, Ph-b), 97.13 (d, C-5), 21.17 (q, CH_3). ESI-HRMS (*m*/*z*): $[M-TsC-Cl]^+$ ($C_{11}H_{11}N_3O_3SCdCl$): calc. 413.9243, found: 413.9225 (4.3 ppm); $[M-Cl]^+$ ($C_{22}H_{22}N_6O_6S_2CdCl$): calc. 678.9764, found: 678.9730 (5.0 ppm); $[M+TsC-Cl]^+$ ($C_{33}H_{33}N_9O_9S_3CdCl$): calc. 944.0286, found: 944.0291 (0.5 ppm).

2.3.3. Co(1-TsC-N3)$_2$Cl$_2$ (**5**)

Starting materials: solutions of 1-(*p*-toluenesulfonyl)cytosine (**1**) (130 mg, 0.5 mmol) in methanol (40 mL), $CoCl_2 \times 6H_2O$ (60 mg, 0.25 mmol) in methanol (4 mL). The resulting dark violet solution was left to slowly evaporate at room temperature yielding 112 mg of blue powder **5**: ^{1}H NMR (DMSO-d_6) δ/ppm: 8.10 (d, 1H, $J_{6,5}$ = 8 Hz, H-6), 7.90 (brd, 2H, NH_2), 7.84 (d, 2H, $J_{b,c}$ = 8.4 Hz, Ph-b), 7.44 (d, 2H, $J_{c,b}$ = 8.4 Hz, Ph-c), 5.93 (d, 1H, $J_{5,6}$ = 7.9 Hz, H-5), 2.40 (s, 3H, CH_3); ^{1}H NMR (CD_3CN) δ/ppm: 8.05 (brd, 1H, H-6), 7.85 (brd, 2H, Ph-b), 7.40 (brd, 2H, Ph-c), 6.33 (brs, 2H, NH_2), 2.42 (brs, 3H, CH_3). ESI-HRMS (*m*/*z*): $[M-Cl]^+$ ($C_{22}H_{22}N_6O_6S_2CoCl$): calc. 624.0063, found: 624.0041 (3.5 ppm); $[M+TsC-Cl]^+$ ($C_{33}H_{33}N_9O_9S_3CoCl$): calc. 889.0584, found: 889.0582 (0.2 ppm).

2.3.4. Cu(1-MsC-N3)$_2$Cl$_2$ (**7**)

Starting materials: solutions of 1-methanesulfonylcytosine (**6**) (113 mg, 0.6 mmol) in methanol (40 mL), $CuCl_2 \times 2H_2O$ (51 mg, 0.3 mmol) in methanol (2 mL). The resulting turquoise solution was left to slowly evaporate at room temperature in order to obtain high quality single crystals. After 5 days, dark green prisms were obtained, one of which was picked for X-ray diffraction measurements, while the others were filtered off, yielding 137 mg (89%) of dark green powder **7**: ^{1}H NMR (DMSO-d_6) δ/ppm: 7.97 (brs, 2H, NH_2), 7.32 (brs, 1H, H-6), 3.67 (s, 3H, CH_3); ^{13}C NMR (DMSO-d_6) δ/ppm: 136.06 (d, C-6), 39.01 (q, CH_3). ESI-HRMS (*m*/*z*): $[M-Cl]^+$ ($C_{10}H_{14}N_6O_6S_2CuCl$): calc. 475.9401, found: 475.9388 (2.7 ppm).

2.3.5. Cd(1-MsC-N3)$_2$Cl$_2$ (**8**)

Starting materials: solutions of 1-methanesulfonylcytosine (**6**) (113 mg, 0.6 mmol) in methanol (40 mL), 2 M aqueous solution of $CdCl_2$ (0.15 mL, 0.3 mmol). After 1 h, a white precipitate was formed. It was filtered off and dried in vacuum to give 131 mg (77%) of snow-white powder **8**. The mother liquor was left to crystallize, but the colorless prisms formed after four days turned out to be single crystals of ligand **6**. Complex **8**: ^{1}H NMR (DMSO-d_6) δ/ppm: 7.92 (brs, 1H, NH), 7.89 (brs, 1H, NH), 7.84 (d, 1H, $J_{6,5}$ = 7.8 Hz, H-6), 5.90 (d, 1H, $J_{5,6}$ = 7.8 Hz, H-5), 3.62 (s, 3H, CH_3); ^{13}C NMR (DMSO-d_6) δ/ppm: 166.06 (s, C-4), 152.08 (s, C-2), 139.08 (d, C-6), 96.68 (d, C-5), 41.05 (q, CH_3). ESI-HRMS (*m*/*z*): $[M-Cl-HCl]^+$ ($C_{10}H_{13}N_6O_6S_2Cd$): calc. 490.9372, found: 490.9345

(5.5 ppm); $[M-Cl-HCl+TsC]^+$ ($C_{15}H_{20}N_9O_9S_3Cd$): calc. 679.9580, found: 679.9556 (3.5 ppm).

2.4. X-ray structural analysis

Crystal data, data collection and refinement parameters are summarized in Table 1. Data collections were performed on an Enraf Nonius CAD4 diffractometer using graphite monochromated Cu Kα radiation (λ = 1.54179 Å) (structures **2**, **3** and **4**) and on an Oxford Diffraction Xcalibur Nova R diffractometer with a microfocusing Cu tube (structures **6** and **7**). The X-ray structure of ligand **1** was reported in our previous paper [6]. Data reduction and cell refinement were carried out using the procedures incorporated into the WINGX package [9] for structures **2**, **3** and **4**, while, CRYSALIS software [10] was used for the structures **6** and **7**. Intensities were measured at room temperature. All structures were solved using direct methods with SIR2002 [11] and refined using full matrix least-squares refinement based on F^2, with SHELX97 [12]. Molecular illustrations were prepared with ORTEP-3 [13] and PLATON [14]. All non-hydrogen atoms in the structures were refined anisotropically and hydrogen atoms were included in their geometrically calculated positions (except for some hydrogen atoms included in hydrogen bonding), and refined according to the riding model.

3. Results and discussion

3.1. Synthesis

The organic ligands were synthesized by procedures described in the literature [7,8]. Condensation of silylated cytosine with *p*-toluenesulfonyl chloride (TsCl) or methanesulfonyl chloride (MsCl) gave the corresponding ligands 1-tosylcytosine, **1** (1-TsC), and 1-mesylcytosine, **6** (1-MsC). The mononuclear complexes described in this paper were prepared by the reaction of Cu(II), Cd(II) and Co(II) chlorides with the corresponding ligands in a 1:2 molar ratio of reactants in methanol and led to complexes of the $M(L)_2Cl_2$ type (Scheme 1).

Two forms of copper complexes with the 1-tosylcytosine ligand **1** were isolated in the process of crystal growth from a diluted methanolic solution: Cu(1-TsC-*N*3)$_2$Cl$_2$ (**2**) and its solvated pseudopolymorph Cu(1-TsC-*N*3)$_2$Cl$_2$ × 2CH$_3$OH (**3**), with suitable monocrystals for X-ray diffraction studies. Crystals suitable for X-ray crystallography were also obtained in the reaction of copper(II) chloride with 1-mesylcytosine **6**, yielding the complex Cu(1-MsC-*N*3)$_2$Cl$_2$ (**7**), and yielding the complex Cd(1-TsC-*N*3)$_2$Cl$_2$ (**4**) in the reaction of cadmium(II) chloride with 1-tosylcytosine **1**. On the other hand, the IR and NMR studies suggested the existence of the Co(II) complex with ligand **1** and the Cd(II) complex with ligand **2**, for which we assume them to be the N3 coordinated species Co(1-TsC-*N*3)$_2$Cl$_2$ (**5**) and Cd(1-MsC-*N*3)$_2$Cl$_2$ (**8**); their molecular formulas were confirmed by HRMS spectrometry.

3.2. NMR Spectroscopy

In the ^{1}H NMR spectrum (measured in DMSO-d_6), complex Cd(1-TsC-*N*3)$_2$Cl$_2$ (**4**) displays a slight downfield shift of the signals for two sets of doublets in the aromatic region corresponding to the H-6 and H-5 protons (δ 8.22 and 6.06 ppm) and phenyl Ph-b and Ph-c protons (δ 7.88 and 7.48 ppm) relative to the free ligand **1**. The H-6 ($\Delta\delta$ 0.03 ppm), H-5 ($\Delta\delta$ 0.06 ppm) and NH ($\Delta\delta$ 0.28 and 0.16 ppm) signals in the Cd(1-MsC-*N*3)$_2$Cl$_2$ (**8**) complex are slightly shifted to higher frequencies compared to those of the free cytosine ligand **6**, which is in accord with coordination *via* N3. These very small changes are in agreement with other cytosine complexes [15].

NMR peak positions are particularly sensitive to the presence of paramagnetic species and "diamagnetic" ^{1}H NMR spectroscopy has not been applied extensively to Cu(II) and Co(II) coordination complexes because of their paramagnetism, which complicates the spectra acquisition and interpretation. On the other hand, almost all signals for complexes Cu(1-TsC-*N*3)$_2$Cl$_2$ (**2**), Co(1-TsC-*N*3)$_2$Cl$_2$ (**5**) and Cu(1-MsC-*N*3)$_2$Cl$_2$ (**7**) were registered in the "diamagnetic" (in the range δ = 0–14 ppm) part of the ^{1}H NMR spectra, showing broad resonances (doublets collapsed into broad singlets). The

Table 1
Crystallographic parameters for compounds **2**, **3**, **4**, **6**, and **7**.

Compound	**2**	**3**	**4**	**6**	**7**
Formula	$C_{22}H_{22}Cl_2CuN_6O_6S_2$	$C_{22}H_{22}Cl_2CuN_6O_6S_2 \times 2CH_3OH$	$C_{22}H_{22}Cl_2CdN_6O_6S_2$	$C_5H_7N_3O_3S$	$C_{10}H_{14}Cl_2CuN_6O_6S_2$
Formula weight (g mol^{-1})	665.02	727.08	713.88	189.2	512.8
Crystal color and habit	blue plate	turquoise plate	colorless prism	colorless prism	green prism
Crystal dimensions (mm)	0.25 × 0.11 × 0.09	0.25 × 0.15 × 0.10	0.25 × 0.18 × 0.15	0.20 × 0.18 × 0.15	0.12 × 0.10 × 0.10
Space group	*P*21/*c*	*P*21/*n*	*P*-1	$P2_1/n$	$P2_1/c$
a (Å)	11.909(2)	14.244(1)	8.7910(3)	5.1275(3)	22.1814(3)
b (Å)	13.247(2)	14.096(1)	13.0760(5)	24.675(1)	7.0616(1)
c (Å)	8.7883(8)	16.003(2)	13.3430(4)	6.3307(5)	12.4291(2)
α (°)	90.00	90.00	113.641(3)	90.00	90.00
β (°)	100.44(2)	104.75(1)	97.747(3)	106.32(1)	103.152(1)
γ (°)	90.00	90.00	97.840(3)	90.00	90.00
V (Å^3)	1363.5(3)	3107.3(5)	1361.25(9)	768.68(9)	1895.78(5)
Z	2	4	2	4	4
μ (Cu Kα) (mm^{-1})	4.803	4.317	10.105	3.567	6.680
Absorption correction	Ψ-scan	Ψ-scan	Ψ-scan	multi-scan	multi-scan
θ max (°)	76.59	76.18	76.39	75.88	76.24
hkl	0,15; −16,16; −11,10	−17,17; −17,0; −20,0	−10,11; −16,0; −15,16	−6,6; −29,30; −7,7	−27,26; −8,8; −15,15
Number of reflections collected	5856	6725	5958	4440	10 263
Number of reflections unique	2865	6493	5702	1593	3881
Number of reflections observed [$I > 2\sigma(I)$]	2474	4430	5106	1534	3357
R_{int}	0.0417	0.0357	0.0194	0.0162	0.0232
R_σ	0.0380	0.0453	0.0256	0.0135	0.0211
Parameters	187	404	384	126	262
R_1 [$I > 2\sigma(I)$]	0.0421	0.0649	0.0415	0.0356	0.0354
R_1, all	0.0491	0.1058	0.0479	0.0364	0.0410
wR_2	0.1134	0.1970	0.1168	0.1152	0.1023
Goodness-of-fit, *S*	1.095	1.067	1.025	1.081	1.081
ρ_{max}, ρ_{min} (e Å^{-3})	0.53, −0.77	0.88, −0.65	1.37, −1.77	0.27, −0.28	0.79, −0.55

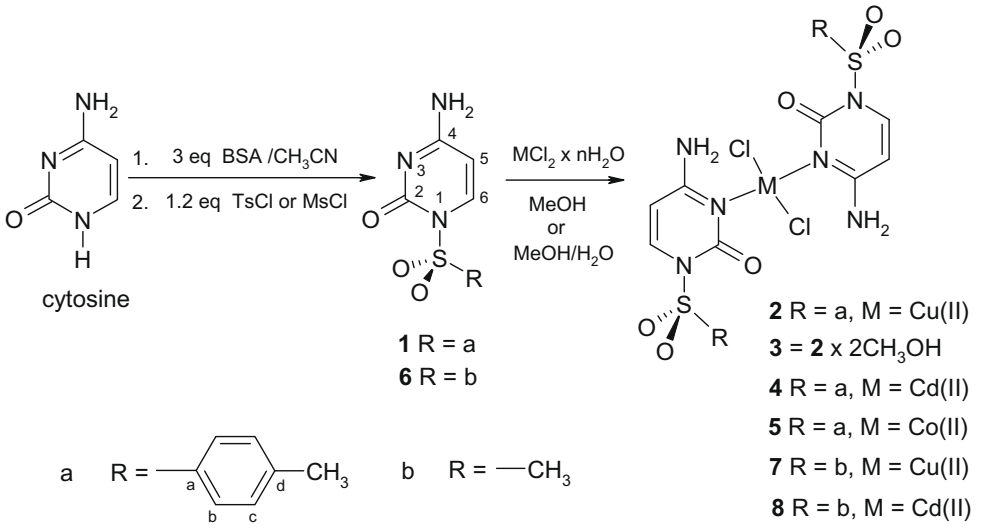

Scheme 1.

signal of H-5, a proton of the cytosine moiety, which is not in the nearest neighborhood to the coordination center, disappeared from the range of "diamagnetic" spectra for complexes **2**, **5** and **7** (*Figs.* S13 and S14 Supplementary material).

The spectrum of complex Co(1-TsC-*N*3)$_2$Cl$_2$ (**5**) exhibits signals of the free ligand **1** in DMSO-d_6 solution (*Figs.* S13), indicating low stability of the complex in polar coordinative solvent. However, the ^{1}H NMR spectrum of **5** measured in CD_3CN shows the disappearance of the H-5 signal, as can be seen for the paramagnetic Cu(II) complex **2**; all other broad resonances are slightly shifted to higher field compared to the spectrum of the free ligand **1** (*Figs.* S14). Due to the lack of an X-ray structure for the Co(II) complex **5**, we can only suggest that the binding probably takes place at the N-3 atom of the cytosine moiety.

3.3. Infrared spectroscopy

The infrared spectra of the free ligands, 1-tosylcytosine **1** and 1-mesylcytosine **6**, together with their complexes with copper, cadmium and cobalt, are shown in Figs. 1 and 2, while the band assignments are given in Table 2. Direct evidence of complexation is the presence of absorption bands due to the metal–chlorine stretching vibration in the spectral region below 500 cm^{-1}. In the region corresponding to ν(NH) vibrations, the spectra of 1-tosylcytosine **1** and 1-mesylcytosine **6** undergo prominent changes due to complexation, both in the band positions and intensities.

3.4. The molecular and crystal structures of 1-tosylcytosine complexes *2*, *3* and *4*

The molecular structures of the Cu(II) complexes, pseudopolymorphs **2** and **3**, as well as of the Cd(II) complex **4** are given in Figs. 3–5, respectively. The geometries of the pyrimidine rings in complexes **2**, **3** and **4** are given in Table 3. As the Cu(II) ion in complex **2** lies on an inversion center, and consequently the molecule possesses C_i symmetry, the two cytosine rings have identical geometries. This is, however, not the case of complexes **3** and **4**. Moreover, in the cytosine ring 1 (cy1) of complex **3**, the values of bond lengths N3–C4 and C4–N4 suggest an increase of the single bond character of the former, and an increase of the double bond character of the latter, compared to complexes **2** and **4** as well as to the other cytosine ring (cy2) of the same complex (Table 3). They

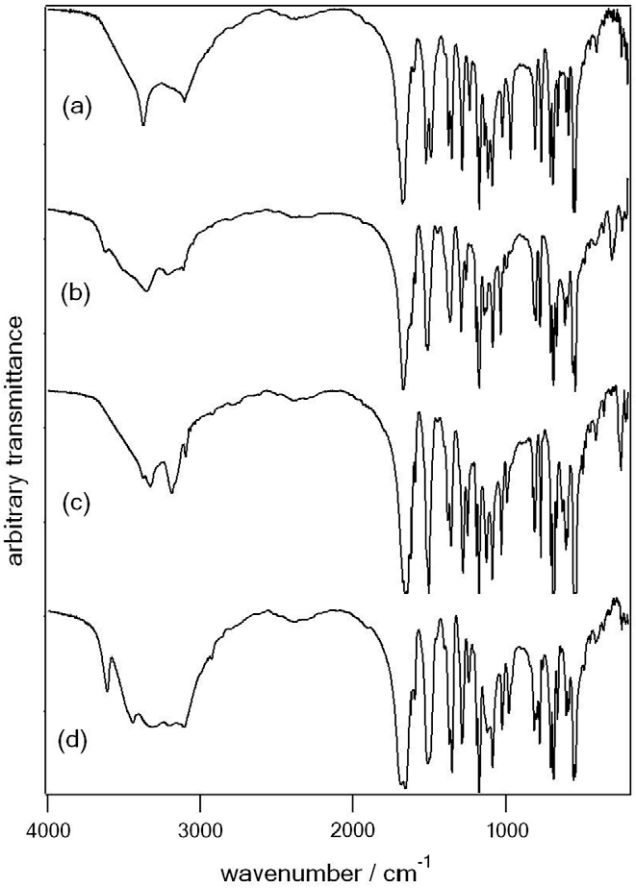

Fig. 1. Infrared spectra of (a) 1-tosylcytosine **1**, (b) Cu(1-TsC-*N*3)$_2$Cl$_2$ x 2CH$_3$OH (**3**), (c) Cd(1-TsC-*N*3)$_2$Cl$_2$ (**4**) and (d) Co(1-TsC-*N*3)$_2$Cl$_2$ (**5**).

are, in fact, in very good accord with the analogous average values extracted from the current version of *CSD* [16] for a set of 14 structures containing the iminooxo form of *N*-1-substituted cytosine [N3–C4, 1.359(5) Å; C4–N4, 1.300(4) Å]. This is due to charge delocalization over the bonds N3–C4 and C4–N4, caused by the copper coordination. Search of the same version of the *CSD* has revealed

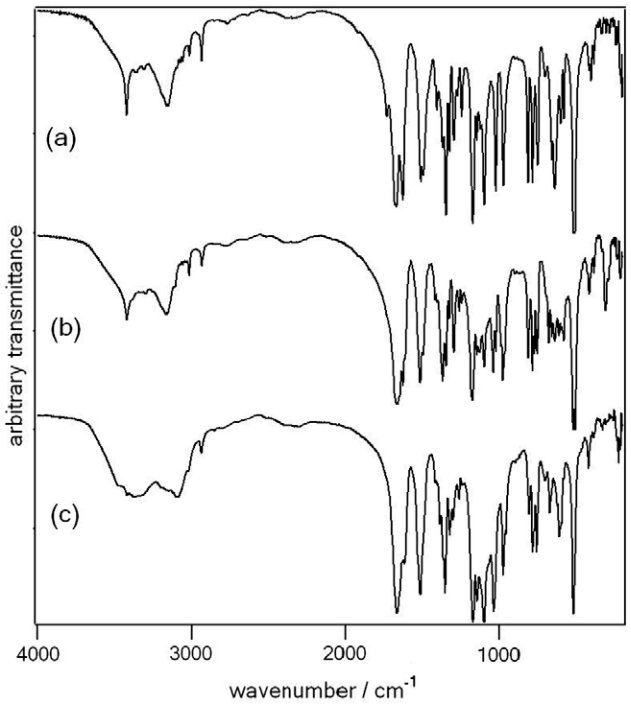

Fig. 2. Infrared spectra of (a) 1-mesylcytosine **6**, (b) Cu(1-MsC-*N*3)$_2$Cl$_2$ (**7**) and (c) Cd(1-MsC-*N*3)$_2$Cl$_2$ (**8**).

291 structures containing the preferred amino-oxo form of *N*-1-substituted cytosine. In this set, the average values for these bond lengths are: N3–C4, 1.346(1) Å, and C4–N4, 1.323(1) Å, which correspond to the analogous values in complexes **2** and **4**, and also, approximately, to the bond lengths revealed by the cytosine ring 2 (cy2) of complex **3**.

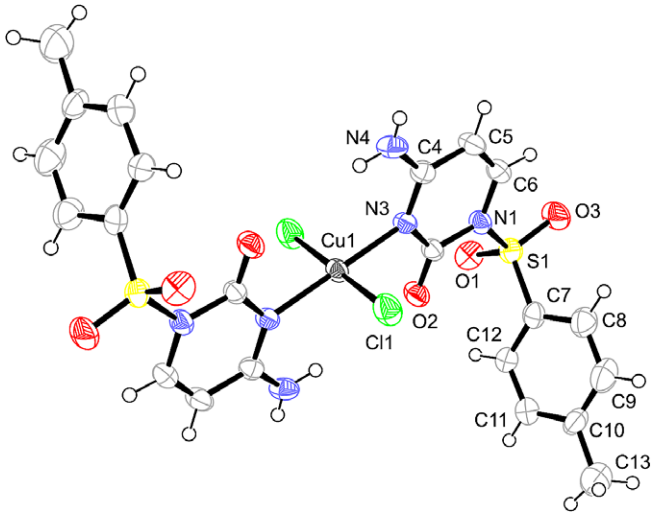

Fig. 3. ORTEP drawing of **2**. Thermal ellipsoids are scaled at the 50% probability level.

In both copper complexes **2** and **3**, the central ion forms a square-planar coordination sphere, almost ideal in the case of **2**, and considerably distorted in the case of **3** (Table 4). On the other hand, while the two coordinated pyrimidine rings are in a *trans*-arrangement with respect to the central Cu(II) ion [N3–Cu1–N3*i*, 180(11)°, see Table 4] and are virtually coplanar (head-to-tail oriented), they are mutually *cis*-oriented in complex **3** [N3–Cu1–N23, 90.88(14)°, see Table 4], and their corresponding *ls* planes

Table 2
Characteristic infrared bands (wavenumbers in cm^{-1}) in the 4000–200 cm^{-1} range and with tentative band assignments.

1	3	4	5	6	7	8	Assignation
	3621 w[a]						Adsorbed MeOH ν(OH)
			3608 m[b]				Adsorbed water ν(OH)
3372s	3355 s, b	3374 s	3441 s	3418 s	3418 s	3369 s, b	ν_{asym}(NH)
		3325 m	3311 s	3358 m	3381 sh		ν(NH)
				3306 m	3300 w	3318 w, b	ν(NH)
3186 w, sh	3217 m	3186 m	3200 m	3188 w, sh	3193 w, sh	3192 m	ν(NH)
3101 m	3109 m	3091 m	3100 m	3155 s	3162 s	3102 s	ν_{sym}(NH)
				3096 m	3110 m		ν(NH)
1702 m, sh				1729 m			δ(NH$_2$)
1673 vs	1667 vs	1671 vs	1684 vs	1677 vs	1663 vs	1663 vs	ν(C=O)
1662 vs	1647 m, sh	1656 vs	1655 vs	1668 vs	1650 s, sh	1648 s, sh	ν(C=C), ν(C=N), δ(NH$_2$)
1648 m, sh	1620 m, sh	1641 vs		1655 w, sh			ν(ring), ν(C=N), δ(NH)
1601 m	1596 m	1623 m, sh	1596 m	1626 s	1626 s	1629 vs	δ(NH)
		1595 m					δ(NH)
1523 s	1511 s	1506 s	1512 s	1509 s	1513 s	1511 s	ν(ring), ν(C–NH$_2$), δ(NH)
1490 s			1499 s	1493 s	1496 m		δ(NH), ν(C–N), ν(ring), δ(CH)
1377 m	1379 m, sh	1380 m	1371 s	1366 m	1365 s	1362 m	ν(SO$_2$)
1354 s	1367 m	1359 m	1353 s	1345 s	1344 s	1350 s	ν(SO$_2$)
1286 s	1293 s	1281 s	1287 s	1293 s	1294 s	1298 m	Cytosine breathing
1186 m	1194 m		1191 s		1180 m		ν_{ring}
1174 s	1173 s	1177 s	1175 vs	1171 s	1172 m	1171 m	ν_{ring}
1139 m	1142 m	1137 w, sh	1137 w, sh	1145 m	1145 m	1143 m	ρ(NH$_2$)
765 m	774 m	770 m	775 s		775 s	775 w, sh	γ(NH$_2$)
554 s	557 s	549 s	554 vs	520 s	523 s	520 s	τ(NH$_2$)
542 s	543 s	538 s	542 vs		509 s		τ(NH$_2$)
				387 m	387 m	389 m	δ(CO) or δ(CN)
	302 m	249 m	227 w		311 m	227 m	ν(MCl)

vs: very strong; s: strong; m: medium; w: weak: stretching; : deformation; γ: out-of-plane bending; τ: torsion.
M: Cu(II) (complexes **3** and **7**); Cd(II) (complexes **4** and **8**); Co(II) (complex **5**).

[a] Thermogravimetry of **3** shows a continuous mass loss of 6.45%. This, together with the IR band position, shows that methanol is only weakly adsorbed to the crystal of **3** (Figs. S1a).

[b] The thermogram of the complex **5** reveals a continuous mass loss of 2.66%, which corresponds to one water molecule per formula unit. This, together with the IR band position, indicates that water is only weakly adsorbed to the crystal of **5** (Figs. S1b).

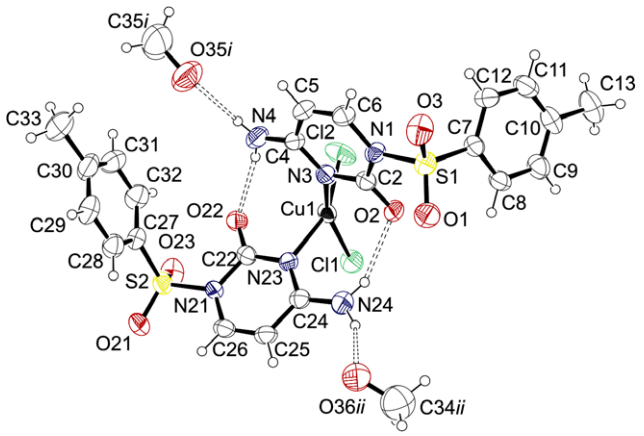

Fig. 4. ORTEP drawing of **3**. Thermal ellipsoids are scaled at the 40% probability level Hydrogen bonds are given by dashed lines.

form an angle of 72.5(2)°. The crystal structure of **2** is characterized by a complex three-dimensional hydrogen bonded molecular network where each complex molecule is connected to two others through amino-group protons forming hydrogen bonds towards O2*i* and O3*i* of the neighboring molecule (Table 5a and Fig. 6). The crystal packing is less complicated by far in the structure of complex **3**, where a single complex molecule is connected through intermolecular hydrogen bonds to only two neighboring solvent molecules, forming with them discrete hydrogen bonded units (Table 5a and Fig. 4). The refinement of the OH group hydrogens of both solvent molecules does not converge, and consequently they are not included in the model. They might however extend the hydrogen bonding network in this structure.

Table 4
Geometry of the coordination spheres in complexes **2**, **3**, **4**, and **7**.

	2	**3**	**4**	**7**
Bond (Å)				
M–N3	1.988(2)	2.033(4)	2.260(3)	2.0176(19)
M–N3*i* (N23)	1.988(2)	2.030(3)	2.278(3)	2.0333(19)
M–Cl1	2.2547(7)	2.2349(14)	2.4490(10)	2.2173(8)
M–Cl1*i* (Cl2)	2.2547(7)	2.2216(15)	2.4707(9)	2.2267(8)
Angle (°)				
N3–M–N3*i* (N23)	180.00(11)	90.88(14)	129.66(11)	91.21(8)
N3–M–Cl1	90.76(6)	157.87(11)	101.19(8)	91.12(6)
N3–M–Cl1*i* (Cl2)	89.24(6)	91.04(11)	108.37(8)	156.54(6)
N3*i* (N23)–M–Cl1	89.24(6)	90.23(10)	107.84(8)	161.08(7)
N3*i* (N23)–M–Cl1*i* (Cl2)	90.76(6)	156.70(11)	98.95(8)	88.29(6)
Cl1–M–Cl1*i* (Cl2)	180.00(3)	96.59(6)	110.33(4)	96.90(4)

Complex **4** is a neutral complex where the positive charge of the central Cd(II) ion is compensated by two chlorine anions, forming together with two endocyclic N3 atoms that belong to cytosine rings of the two ligand molecules a slightly distorted tetrahedral coordination sphere (Table 4 and Fig. 5). Its crystal structure is characterized by a complex hydrogen bonded three-dimensional molecular network. Two ligand molecules coordinated to the central Cd(II) ion form different hydrogen bonds *via* their amino groups, thus creating an asymmetric environment around the Cd(II) cation (Table 5a). While cytosine 1 of complex **4** forms one intramolecular H-bond *via* N4-H4A, and one intermolecular hydrogen bond with the chlorine from the neighboring molecule *via* N4-H4B, cytosine 2 forms, besides these two hydrogen bonds, an

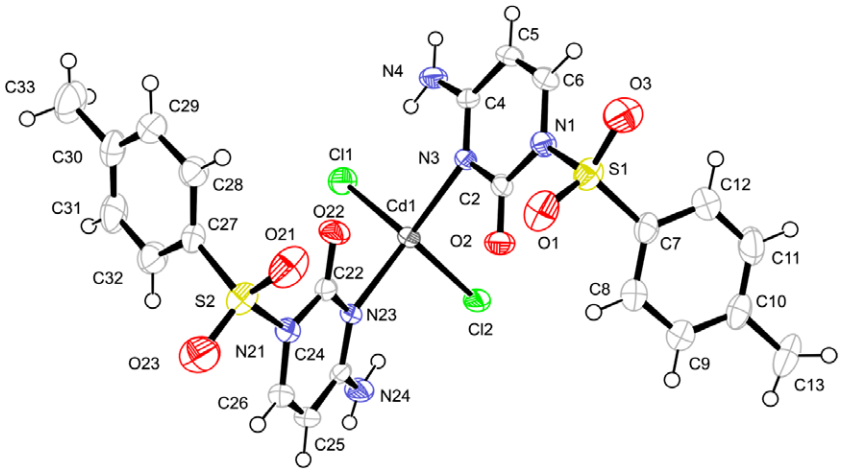

Fig. 5. ORTEP drawing of **4**. Thermal ellipsoids are scaled at the 50% probability level.

Table 3
Bond distances in the cytosine ring (Å).

Bond	**2**	**3** (cy1)	**3** (cy2)	**4** (cy1)	**4** (cy2)	**6**	**7** (cy1)	**7** (cy2)
N1–C2	1.409(3)	1.400(6)	1.410(6)	1.412(4)	1.403(5)	1.433(2)	1.394(3)	1.404(3)
C2–O2	1.222(3)	1.228(6)	1.223(6)	1.214(5)	1.224(5)	1.227(2)	1.237(3)	1.226(3)
C2–N3	1.360(3)	1.351(6)	1.349(6)	1.362(5)	1.360(5)	1.341(2)	1.344(3)	1.349(3)
N3–C4	1.339(3)	1.355(6)	1.328(6)	1.339(4)	1.338(4)	1.337(2)	1.345(3)	1.333(3)
C4–N4	1.320(4)	1.299(7)	1.310(7)	1.319(5)	1.320(5)	1.317(2)	1.310(4)	1.313(4)
C4–C5	1.428(4)	1.417(7)	1.440(7)	1.436(5)	1.435(5)	1.437(2)	1.426(4)	1.432(4)
C5–C6	1.333(4)	1.316(8)	1.323(8)	1.335(6)	1.329(6)	1.323(2)	1.318(4)	1.327(4)
C6–N1	1.383(3)	1.383(6)	1.375(7)	1.377(5)	1.378(5)	1.391(2)	1.388(3)	1.383(3)

Table 5a
Hydrogen bonds in 1-tosylcytosine complexes **2**, **3** and **4**.

D–H···A	*d* (D–H)/Å	*d* (H···A)/Å	*d* (D···A)/Å	∠ (D–H···A)/°	Symm. operation
Complex ***2*** *[Cu(1-TsC-N3)$_2$Cl$_2$]*					
N4–H4A···O3*i*	0.86(4)	2.49(4)	2.991(3)	118(3)	(*i*) −*x*, 1/2 + *y*, 1/2 − *z*
N4–H4B···O2*i*	0.72(4)	2.41(4)	3.086(3)	157(4)	(*i*) −*x*, 1/2 + *y*, 1/2 − *z*
Complex ***3*** *[Cu(1-TsC-N3)$_2$Cl$_2$ × 2CH$_3$OH]*					
N4–H4A···O35*i*	0.76(6)	2.21(6)	2.951(9)	166(6)	(*i*) 1 − *x*, −*y*, −*z*
N4–H4B···O22	0.80(6)	2.24(6)	2.986(7)	156(6)	
N24–H24A···O2	0.79(10)	2.30(10)	3.031(7)	153(9)	
N24–H24B···O36*ii*	0.81(7)	2.07(7)	2.847(9)	159(7)	(*ii*) 1 − *x*, −*y*, 1 − *z*
Complex ***4*** *[Cd(1-TsC-N3)$_2$Cl$_2$]*					
N4–H4A···Cl1	0.90(7)	2.36(7)	3.247(4)	168(5)	
N4–H4B···Cl2*i*	0.90(6)	2.44(6)	3.296(4)	158(5)	(*i*) −*x*,1 −*y*, −*z*
N24–H24A···Cl2	0.93(8)	2.61(8)	3.371(4)	139(6)	
N24–H24A···O21*ii*	0.93(8)	2.40(7)	3.141(5)	136(6)	(*ii*) −1 + *x*, *y*, *z*
N24–H24B···Cl2*iii*	0.79(7)	2.51(6)	3.273(4)	164(5)	(*iii*) −*x*, 2 − *y*, −*z*

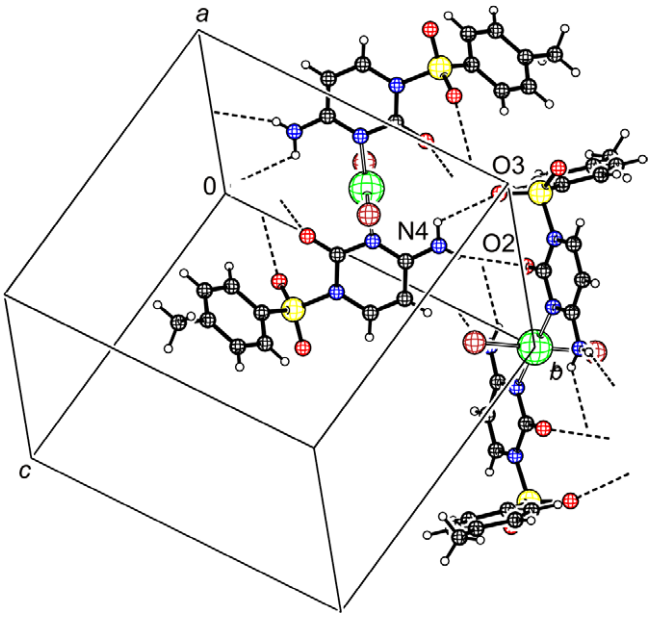

Fig. 6. Crystal packing of **2**.

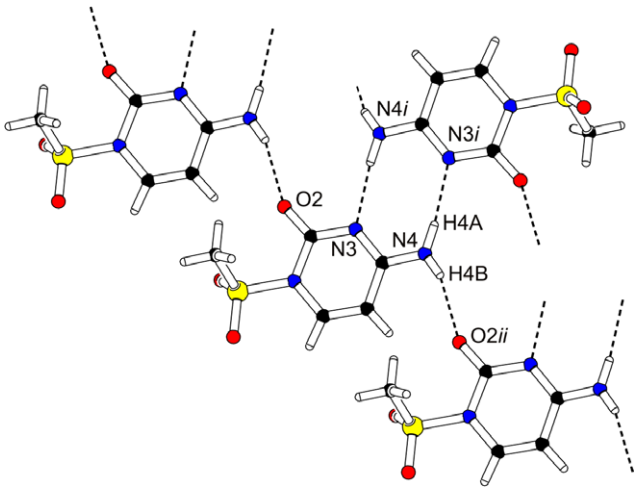

Fig. 7. Hydrogen bonding in **6**.

additional hydrogen bond N24–H24A···O21*ii*, thus creating a bifurcated hydrogen bond *via* the H24A proton.

*3.5. The molecular and crystal structures of 1-mesylcytosine **6** and its Cu(II) complex **7***

The hydrogen bonding pattern of ligand **6** is given in Fig. 7. The molecular structure of this ligand reveals no unexpected features. The geometry of the pyrimidine ring is typical of an N1-substituted cytosine in the preferred aminooxo form [6]. The hydrogen bonding pattern (Table 5b) reveals centrosymmetric dimers formed by the H-bond N4–H4A···N3*i*. These dimers are further connected into endless chains *via* the N4–H4B···O2*ii* hydrogen bond. The ORTEP drawing of complex **7** is given in Fig. 8 and its crystal packing is displayed in Fig. 9. In complex **7**, the Cu(II) ion resides in the center of a rather unusual, severely distorted coordination sphere that could be described as a transition state between a square planar and a tetrahedral arrangement, and strongly resembles the coordination sphere of Cu(II) in complex **3**. Relevant geometry parameters are given in Table 4. Both of these complexes lack molecular C_i symmetry, unlike complex **2** where the central Cu(II) ion lies on an inversion center and reveals a square-planar coordination sphere. Four ligand atoms (N3, N23, Cl1 and Cl2) reveal strong deviations from the *ls* plane calculated through them and the central Cu(II) ion, with the average absolute value of 0.38(2) Å. The angle between the planes defined by Cl1, Cu1 and Cl2 and by N3, Cu1 and N23 is 28.97(4)°. These values describe the coordination sphere of complex **7** as a severely distorted square plane, rather than as a severely distorted tetrahedron. Angles N3–Cu1–N23 and Cl1–Cu1–Cl2 [91.21(8)° and 96.26(4)°, see Table 4] further support this conclusion and, moreover, suggest a *cis*-arrangement. An obvious result is the angle of 73.56(6)° formed by the *ls* planes of two pyrimidine rings, which are, hence, close to a mutual perpendicular arrangement, similarly as in complex **3**, and unlike in complex **2**, where the two pyrimidine rings are coplanar and *trans* oriented with respect to the central Cu(II) ion (*vide supra*). The crystal structure of **7** is characterized by endless hydrogen bonded molecular chains along the crystallographic *b* axis (Fig. 9). These chains are formed by the N4–H4A···O2*i* hydrogen bond (Table 5b). Through its remaining hydrogen, H4B, N4 forms an intramolecular hydrogen bond, N4–H4B···O22, symmetrical (with respect to Cu(II)) with the hydrogen bond N24–H24B···O2 (Fig. 8). Hence, O2 acts as a double acceptor, taking part in one intramolecular and one intermolecular hydrogen bond. Nevertheless, two exocyclic nitrogen atoms from two cytosine rings, N4 and N24, reveal an asymmetrical hydrogen bonding pattern. N4 forms an intermolecular bond to O2*i* and an intramolecular one to O22 (*vide supra*), while N24 forms an intramolecular hydrogen bond to O2, and an

Table 5b
Hydrogen bonds in 1-mesylcytosine **6** and its Cu(II) complex **7**.

D–H···A	*d* (D–H)/Å	*d* (H···A)/Å	*d* (D···A)/Å	∠ (D–H···A)/°	Sym. operation
Ligand ***6*** *(MsC)*					
N4–H4A···N3*i*	0.90(2)	2.04(2)	2.938(2)	175(2)	(*i*) 1 − *x*, −*y*, 2 − *z*
N4–H4B···O2*ii*	0.80(2)	2.24(2)	3.011(2)	162(2)	(*ii*) *x* − 1, *y*, *z* − 1
Complex ***7*** *[Cu(1-MsC-N3)$_2$Cl$_2$]*					
N4–H4A···O2*i*	0.80(3)	2.27(4)	3.056(2)	167(1)	(*i*) *x*, −1 + *y*, *z*
N4–H4B···O22	0.76(2)	2.23(5)	2.950(3)	157(1)	
N24–H24A···Cl2*ii*	0.85(5)	2.33(8)	3.172(4)	171(1)	(*ii*) *x*, 5/2 − *y*, −1/2 + *z*
N24–H24B···O2	0.81(4)	2.23(7)	2.998(6)	159(1)	

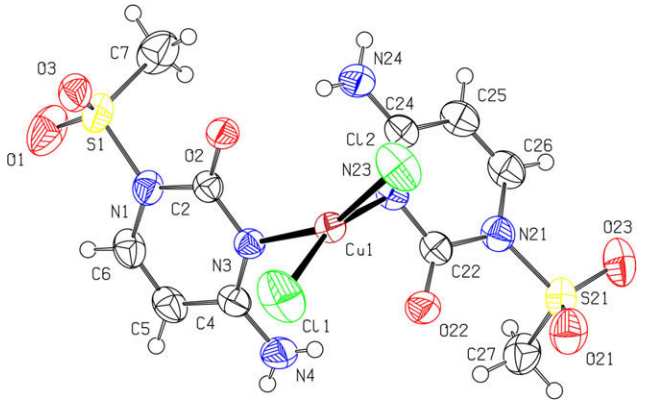

Fig. 8. ORTEP drawing of **7**. Thermal ellipsoids are scaled at the 50% probability level.

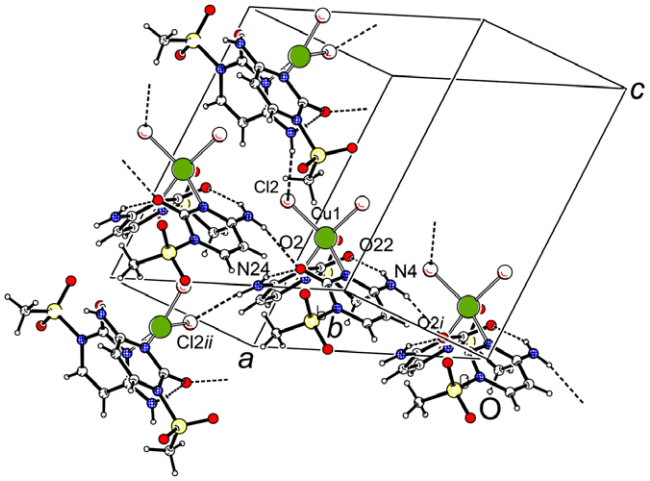

Fig. 9. Crystal packing of **7**.

intermolecular bond N24–H24a···Cl*ii* through which the above described molecular chains along the crystallographic *b* axis are interconnected, forming a two-dimensional molecular grid which propagates parallel to the *bc* plane. A narrow *zig-zag* channel separates two neighboring grids.

4. Conclusions

The mononuclear complexes of the type M(L$_2$)Cl$_2$ described in this paper were prepared by the reaction of Cu(II), Cd(II) and Co(II) chlorides with the 1-tosylcytosine **1** or 1-mesylcytosine **6** ligands. NMR and IR spectra show clear evidence of the complexation of ligands **1** and **6** with Cu(II) [complexes **3** and **7**], Cd(II) [complexes **4** and **8**] and Co(II) [complex **5**].

Two forms of copper complexes with 1-tosylcytosine ligand **1** were isolated in the process of crystal growth from a diluted methanolic solution: Cu(1-TsC-*N*3)$_2$Cl$_2$ (**2**) and its solvated pseudopolymorph Cu(1-TsC-*N*3)$_2$Cl$_2$ × 2CH$_3$OH (**3**). The X-ray structure of the complex **3** revealed charge delocalization inside the cytosine ring, prompted by metal coordination, which is the first step towards tautomerization. This, to the best of our knowledge, has not been observed previously with the copper complexes of *N*-1 substituted cytosine.

Acknowledgments

We appreciate the financial support of the Ministry of Science, Education and Sports of the Republic of Croatia through Grant Nos. 098-0982914-2935, 098-1191344-2943 and 098-0982904-2927. We also thank Renata Kobetić and Dubravka Gembarovski for HRMS, Ernest Sanders for TG measurements, and Krešimir Molčanov for X-ray data collection for compounds **6** and **7**.

Appendix A. Supplementary data

CCDC 729010, 729011, 729012, 729013 and 729014 contains the supplementary crystallographic data for **2**, **3**, **4**, **6** and **7**. These data can be obtained free of charge via http://www.ccdc.cam.ac.uk/conts/retrieving.html, or from the Cambridge Crystallographic Data Centre, 12 Union Road, Cambridge CB2 1EZ, UK; fax: (+44) 1223-336-033; or e-mail: deposit@ccdc.cam.ac.uk. Supplementary data associated with this article can be found, in the online version, at doi:10.1016/j.poly.2009.06.088.

References

[1] (a) M.A. Salam, K. Aoki, Inorg. Chim. Acta 311 (2000) 15;
(b) L. Jing, Z. Wenchao, H.K. Angela, L. Yi, Nucleic Acids Res. 28 (2000) 481;
(c) A.Y. Louie, T.J. Meade, Chem. Rev. 99 (1999) 2711;
(d) M. Sabat, A. Satyshur, M. Sundaralingam, J. Am. Chem. Soc. 105 (1983) 976.
[2] (a) J. Müller, R.K.O. Sigel, B. Lippert, J. Inorg. Biochem. 79 (2000) 261;
(b) J.C. Verheijen, G.A. van der Marel, J.H. van Boom, N. Metzler-Nolte, Bioconjugate Chem. 11 (2000) 741;
(c) S.J. Lippard, in: I. Bertini, H.B. Gray, S.J. Lippard, J.S. Valentine (Eds.), Bioorganic Chemistry, University Science Books, Mill Valley, CA, 1994, p. 505.
[3] (a) S. Sikova, S.J. Rowan, J. Chem. Soc. Rev. 34 (2005) 9;
(b) J.A.R. Navarro, B. Lippert, Coord. Chem. Rev. 22 (2001) 219;
(c) G. Mukherjee, T. Ghosh, J. Inorg. Biochem. 59 (1995) 827.
[4] V.A. Malkov, O.N. Voloshin, V.N. Soyfer, M.D. Frank-Kamenetskii, Nucleic Acids Res. 21 (1993) 585.
[5] (a) Lj. Glavaš-Obrovac, I. Karner, B. Žinić, K. Pavelić, Anticancer Res. 21 (2001) 1979;
(b) F. Supek, M. Kralj, M. Marjanović, L. Šuman, T. Šmuc, I. Krizmanić, B. Žinić, Invest. New Drugs 26 (2008) 97;
(c) A. Višnjevac, M. Žinić, M. Luić, D. Žiher, T. Kajfež Novak, B. Žinić, Tetrahedron 63 (2007) 86.
[6] A. Višnjevac, M. Luić, R. Kobetić, D. Gembarovski, B. Žinić, Polyhedron 28 (2009) 1057.
[7] J. Kašnar-Šamprec, Lj. Glavaš-Obrovac, M. Pavlak, I. Mihaljević, V. Mrljak, N. Štambuk, P. Konjevoda, B. Žinić, Croat. Chem. Acta 78 (2005) 261.
[8] B. Žinić, M. Žinić, I. Krizmanić, EP 0 877 022 B1 Synthesis of the sulfonylpyrimidine derivatives with anticancer activity, 2003.
[9] L.J. Faruggia, J. Appl. Cryst. 32 (1999) 837.

[10] CrysAlis CCD, Oxford Diffraction Ltd., Version 1.171.32.29 (release 10-06-2008 CrysAlis171 .NET).
[11] M.C. Burla, M. Camalli, B. Carrozzini, G.L. Cascarano, C. Giaccovazzo, G. Polidori, R. Spagna, SIR2002, Version 1.0, A Program for Automatic Solution and Refinement of Crystal Structures, University of Bari, Bari, Italy, 2002.
[12] G.M. Sheldrick, SHELX97: Program for the Refinement of Crystal Structures, Universität Göttingen, Germany, 1997.
[13] L.J. Farrugia, J. Appl. Crystallogr. 30 (1997) 565.
[14] (a) A.L. Spek, Acta Crystallogr., Sect. A 46 (1990) C34;
[b] A.L. Spek, PLATON, A Multipurpose Crystallographic Tool, Utrecht University, Utrecht, The Netherlands, 1998.
[15] (a) T. Pizzino, A. Fontana, F. Maggio, Monatsh. Chem. 121 (1990) 3;
(b) M. Concepcio Capllonch, A. Garcıa-Raso, A. Terron, M. Cristina Apella, E. Espinosa, E. Molins, J. Inorg. Biochem. 85 (2001) 173.
[16] F.H. Allen, Acta Crystallogr., Sect. B 58 (2002) 380.